

Parallelised production of fine and calibrated emulsions by coupling flow-focusing technique and partial wetting phenomenon

Céline Cohen · Rory Giles · Victoria Sergeyeva ·
Nitesh Mittal · Patrick Tabeling · Djamal Zerrouki ·
Jean Baudry · Jérôme Bibette · Nicolas Bremond

Received: 24 June 2013 / Accepted: 4 February 2014 / Published online: 21 February 2014
© Springer-Verlag Berlin Heidelberg 2014

Abstract The capacity of microfluidic technology to fabricate monodisperse emulsion droplets is well established. Parallelisation of droplet production is a prerequisite for using such an approach for making high-quality materials for either fundamental or industrial applications where product quantity matters. Here, we investigate the emulsification efficiency of parallelised drop generators based on a flow-focusing geometry when incorporating the role of partial wetting in order to make emulsion droplets with a diameter below 10 μm . Confinement intrinsically encountered in microsystems intensifies the role played by interfaces between liquids and solids. We thus take advantage of partial wetting to enhance the maximum confinement accessible due to liquid flow focusing. We compare the performances brought by partial

wetting to more established routes such as step emulsification. We show that the step configuration and the partial wetting regime are both well suited for being parallelised and thus open the way to the production of fine and calibrated emulsions for further applications. Finally, this new route of emulsification that exploits partial wetting between the fluids and the channel walls opens possibilities to the formation of substantially smaller droplets, as required in many fields of application.

Keywords Emulsion · Microfluidics · Wetting · Step emulsification · Parallelisation

1 Introduction

The physicochemical mechanisms of emulsification have been the subject of numerous investigations because of the wide appeal of emulsions in both fundamental and applied sciences (Leal-Calderon et al. 2007; Bremond and Bibette 2012). Emulsion drops can act as small compartments for encapsulating molecules, particles or cells and where chemical or biochemical reactions take place (Tawfik and Griffiths 1998; Margulies et al. 2005; Song et al. 2006; Theberge et al 2010; Vyawahare et al. 2010). In such a way, drops are used, for example, as microreactors for the synthesis of solid particles which result from the solidification of the droplet content via chemical reactions, which can be photo-induced or through solvent evaporation (Seo et al. 2005; Dendukuri and Doyle 2009; Vladislavljec et al. 2012a). The advantage of this approach as compared to other techniques based on nucleation and growth processes (Fitch 1997) is the ability to encapsulate various components and thus to make composite materials. Indeed, the dispersed phase can be itself a colloidal dispersion,

C. Cohen · R. Giles · V. Sergeyeva · N. Mittal · J. Baudry ·
J. Bibette · N. Bremond (✉)
Laboratoire Colloïdes et Matériaux Divisés, CNRS UMR 8231,
ESPCI ParisTech, 10 rue Vauquelin, 75231 Paris, France
e-mail: nicolas.bremond@espci.fr

Present Address:

C. Cohen
CNRS UMR 7336, UNSA Univ,
Parc Valrose, 06100, Nice, France

N. Mittal
Ecole Polytechnique (Member of ParisTech),
Palaiseau Cedex 91128, France

P. Tabeling
CNRS UMR 7083, ESPCI ParisTech,
10 rue Vauquelin, 75231 Paris, France

D. Zerrouki
Department of Chemical Engineering,
University of Ouargla, 30000 Ouargla, Algeria

such as a ferrofluid, for example, which could lead to magnetic properties of the final micrometre particles. These magnetic beads find applications from sample preparation (Olsvik et al. 1994) to sequencing (Margulies et al. 2005) and immunoassay (Liabakk et al. 1990). Moreover, the use of emulsion droplet template can easily lead to the synthesis of particles larger than the micrometre size, or for making complex colloidal assemblies (Manoharan et al. 2003; Glotzer and Solomon 2007), janus particles (Hong et al. 2006) or composite colloidal pairs that self-assemble (Zerrouki et al. 2008). Typical emulsification techniques often lead to broad distributions of droplet size since the main physical parameters that control drop formation, like shear, are not homogeneous. For various applications and research fields where emulsion drops are used as template, there is a need to obtain droplet size from 1 to 10 μm in a narrow range, i.e. a polydispersity of a few percents together with well-controlled bulk or interfacial properties.

Microfluidic technology is a promising way to fulfil these requirements. Indeed, it is possible to create drops one by one in a reproducible way with simple or complex internal structures (Shah et al. 2008; Vladisavljevic et al. 2012b). Even though the resulting drop size is a function of bulk and interfacial properties and can be tuned by the flow of the dispersed and continuous phases, it is mainly governed by the geometry of the drop maker (Christopher and Anna 2007). Small microchannel features are thus needed for obtaining fine emulsion droplets. A drawback of this approach is the low production yield since the corresponding liquid flow rates are weak. Parallelisation of drop generators is thus a prerequisite for making large quantities of material. Parallelised drop formation has been demonstrated in microfluidic systems based on standard and accessible microfabrication processes, such as soft lithography techniques, but the resulting drop size is always larger than a few tens of micrometres (Nisisako and Torii 2008; Li et al. 2009; Tetradis-Meris et al. 2009; Romanowsky et al. 2012). Mass production of smaller droplets has been achieved in silicon and glass devices (Kawakatsu et al. 1997; Kobayashi et al. 2002, 2005, 2010) that rely on the principle of membrane emulsification process (Nakashima et al. 2000; Joscelyne and Tragardh 2000) where a pore is modelled by a shallow and narrow microchannel. A parent emulsification process, where the drops are formed at the edge of wide slit made in silicon, has been recently proposed (van Dijke et al. 2009). The main drawback of these approaches based on step emulsification is their limitation to situations where the dispersed phase does not wet solid walls. It is also possible to obtain small droplets without necessarily downscaling the microchannel dimensions using instead an extreme hydrodynamic focusing (Ganan-Calvo et al. 2007; Jeong et al. 2012) or with the

aid of surfactants (Anna and Mayer 2006). The parallelisation of such approaches has not been demonstrated so far. Reaching high levels of monodispersity in parallelised systems is not guaranteed, since individual drop makers, necessarily placed close to each other because of limited space availability, can interact and develop new dynamical regimes and thereby, produce droplets of uncontrolled sizes. Phenomena of this type have been observed in two emitters systems (Barbier et al. 2006). Moreover, as the number of drop makers increases, microfabrication heterogeneities may enhance the polydispersity level, to an extent difficult to anticipate, owing to the intricate relation between droplet sizes, geometry and flow conditions. These issues have not been addressed in the literature yet. Finally, the use of microsystems for emulsion production requires to control the wetting properties of the dispersed phase onto the channel walls as high affinities can inhibit drop formation (Dreyfus et al. 2003; Li et al. 2007). Recently, an unfavourable wetting condition has been overcome using a non-planar geometry of the drop generator (Rotem et al. 2012) but the interplay between wetting and emulsification to tailor fine emulsion droplets has not been investigated hitherto.

In this article, we explore the effects of various confinements due the geometry (step), liquid flow (flow focusing) and interfacial energy (partial wetting) on the resulting emulsification process and the straightforward possibility of parallelisation. We first map out the different regimes of emulsification of a flow-focusing device with a step. Then, we show that a partial and transient wetting of the dispersed phase on solid walls can be beneficial for generating monodisperse droplets with a size that can be comparable to the channel height. Finally, we demonstrate that these two emulsification processes can be parallelised, a condition required for mass production.

2 Materials and methods

The microfluidic devices are fabricated by standard soft lithography techniques (McDonald et al. 2000). The photoresist mould is made by a two steps procedure that results in two channel depths. The ratio between the channel depths is at least equal to 10. The mould is replicated using polydimethylsiloxane (PDMS Sylgard, Dow Corning). Once cured, the elastomer replicate is bonded to a glass plate using oxygen plasma. The microsystem is finally heated for 10 min at 70 °C for improving the bonding strength and then filled with water within 30 min to ensure the PDMS channel surface remains hydrophilic.

The liquid injection is either driven with syringe pumps (PHD 2200, Harvard Apparatus) or pressure control systems (MFCS-100, Fluigent). The experiments on

wetting-assisted emulsification reported in Sect. 3.2 are operated with a flow rate control on the aqueous phase. The flow rate of oil, the dispersed phase, is evaluated from the frequency of drop production and their size. The drop formation dynamics is observed with a high-speed camera (SA3, Photron) mounted on an inverted microscope. The drop size is evaluated from image processing.

The continuous aqueous phase is prepared from ultra pure water with NaCl, at a concentration of 0.1 M, and sodium dodecyl sulphate (SDS, Sigma). The dispersed phase is either fluorocarbon oils (3 M Fluorinert) FC-70 or FC-3283 having a dynamic viscosity η_i of 24 and 1.4 mPa s at 25 °C, respectively, or mineral oil (light oil, Sigma) with a viscosity of 23 mPa s. The surface tension γ between the fluorocarbon oils and pure water is 57 mN/m and drops down to 20 mN/m when SDS is added above the critical micellar concentration found to be around 0.2 wt%. An oil soluble surfactant, span 80 (Fluka), is added to the mineral oil to adjust its wetting properties with respect to the channel walls. The interfacial tension between water and mineral oil is reduced from 49 to 7 mN/m when 1 wt% of Span 80 is incorporated and then to 2 mN/m when 0.1 wt% of SDS is added. The interfacial tensions as well as contact angles are measured with a commercial apparatus (SA100, Krüss). All chemicals are used without further purification.

Ferromagnetic nanocrystals were chemically synthesised according to the co-precipitation method (Wang et al. 2006): FeCl₃ and FeCl₂ were dissolved in 2 M HCl at a molar ratio of 2:1. Upon solubilisation, precipitation was induced by rapid stirring with the dropwise addition of 8 M of aqueous ammonia. The resulting black precipitate was then functionalised by adding oleic acid to the reaction mixture and heating it to 80 °C. After cooling, the particles were collected magnetically and rinsed with ethanol to remove part of oleic acid. The ferrofluid was completed by the addition of mineral oil until an even dispersion was achieved. Aggregates were removed from the ferrofluid by centrifugation.

3 Results and discussion

3.1 Flow focusing with a step

The co-flow of immiscible liquids through a constriction (Ganan-Calvo and Gordillo 2001) is a standard method of drop formation in microfluidics (Anna et al. 2003; Christopher and Anna 2007). While the drop size can be varied by tuning the liquid flows, the width as well as the length of the constriction impact on the drop features (Abate et al. 2009). Moreover, the confinement can stabilise the inner liquid jet against fragmentation. Indeed, for an

axisymmetric geometry, the jet is stabilised thanks to a transition from an absolute to convective instability (Guillot et al. 2007). In the case of microchannels having a rectangular cross-section, the vertical confinement allows the formation of a two-dimensional jet that is stable (Dollet et al. 2008; Humphry et al. 2009). The flattened jet can then break if it recovers a cylindrical cross-section by either decreasing the channel width or by increasing the channel depth. The triggered fragmentation at a step has been exploited for making dense emulsions composed of large drops (Priest et al. 2006) or for the generation of micron size droplets (Malloggi et al. 2010) or even sub-micron droplets (Shui et al. 2011) using shallow channels since the drop size scales with the channel height. The drop formation that occurs at the step is close to the one observed during microchannel emulsification (Kawakatsu et al. 1997), but here the capillary instability is coupled to the outer liquid flow. A theoretical description of the emulsification dynamics with this flow configuration is still lacking.

The emulsification features of a flow-focusing device with a step are now reported. The microsystem is composed of a cross made of shallow channels that are connected to deeper channels, as sketched in Fig. 1. The inner fluid is oil, and the continuous phase is water. The fragmentation diagram of such a drop maker is shown in Fig. 2 in the $\{p_i, p_o\}$ plan where the pressure of the inner fluid p_i and the one of the outer fluid p_o correspond to the pressure of each liquid feeding reservoir, the outlet being at atmospheric pressure. For the diagram reported in Fig. 2, the oil is FC-70 and the continuous phase is water with 1 wt% of SDS. The shallow channel's width w and thickness h_1 are 10 and 2 μm , respectively. The length of the shallow channel, between the cross and the step, is 75 μm . The depth h_2 of the deeper channel after the step is 20 μm and should be at least two times larger than h_1 for leading to a drop size independent on step height (Dangla et al. 2013). Three regimes of drop formation, which are linked to the location of fragmentation, are distinguished. When the pressure p_i of the dispersed phase is increased while the pressure p_o of the continuous phase is kept constant, the drops are first formed at the cross-junction (Fig. 2b). As previously discussed (Christopher and Anna 2007), a regular dripping can be obtained via a squeezing mechanism or by shear-induced breakup that leads to the smallest drop size within this regime. In addition, we note the existence of a multiple dripping mode that gives rise to distinct drop sizes, which is unwanted for practical applications. If now the inner pressure is further increased, the width w_i of the jet also grows since it is linked to the ratio between the inner flow rate q_i to the outer one q_o that are both increasing functions of p_i and p_o , respectively (Humphry et al. 2009). The jet jumps to a stable state once w_i is larger

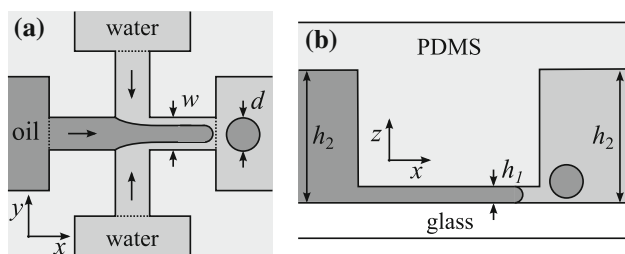


Fig. 1 Sketches of the drop maker geometry in the horizontal plan (a) and vertical plan (b)

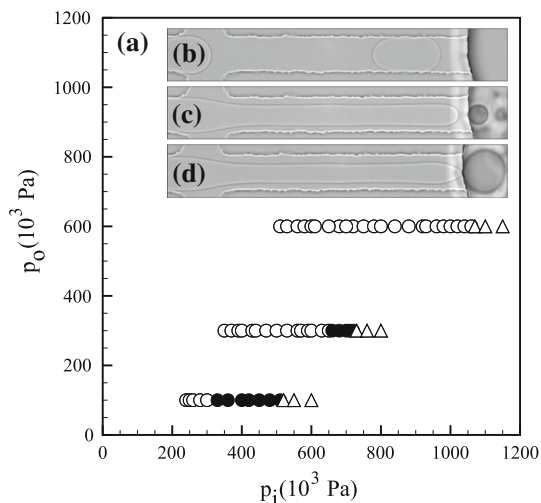


Fig. 2 a Fragmentation diagram of a flow-focusing emulsifier having a step in the $\{p_i, p_o\}$ plan; b dripping at the cross-junction (open circle), c dripping at the step (filled circle), d jetting at the step (triangle). The dispersed phase is a fluorocarbon oil (FC-70), and the continuous phase is water with 1 wt% of SDS. The channel's width w and thickness h_1 are 10 and 2 μm , respectively

that the channel height h_1 and then breaks at the step because of the confinement release (Fig. 2c). Finally, as in membrane emulsification (Sugiura et al. 2002), there exist a critical pressure, and therefore a critical flow rate, beyond which large drops are formed at the step (Fig. 2d). The jump of drop size has been assimilated to a transition from a dripping regime to a jetting regime (Priest et al. 2006). The transition has been observed to occur at a critical capillary number $C_a = q_i \gamma / h_1 w_i \eta_i$ that is a decreasing function of the jet confinement w_i / h_1 prior to the step (Priest et al. 2006).

The step emulsification regime is therefore delimited by the three-dimensional to two-dimensional jet transition at the cross-junction and by the dripping to jetting transition at the step. The cross of the two frontiers defines the maximum outer phase pressure p_o beyond which the step emulsification does not exist anymore. In the step emulsification regime, the drop diameter is almost constant and close to 8 μm and the maximum frequency of drop formation is around 2 kHz. For a less viscous oil (FC-3283),

higher flow rates are accessible before the transition of fragmentation regime that leads to a maximum frequency of 15 kHz. This leads to rather low production yield which varies from 0.002 ml of droplets per hour to 0.015 ml/h. Parallelisation is thus required and will be discussed later on. We now wonder how the wetting properties of the two phases on solid walls modify the fragmentation features.

3.2 Flow focusing with wetting

During emulsification, it is usually necessary to prevent wetting of the dispersed phase onto the container walls. This is especially true for microfluidic systems for which the surface to volume ratio is important and where surface wetting can prohibit emulsion drop formation (Dreyfus et al. 2003). Indeed, when mineral oil is used in the present microsystem, three continuous liquid streams are flowing at the cross and finally form large drops after the step. In this case mineral oil partially wets PDMS and glass after plasma bonding, the contact angle θ of water is around 25° on PDMS and 35° on glass (see Fig. 3 for the definition of θ). When SDS is added to the aqueous outer phase to prevent droplet coalescence, the various fragmentation regimes reported in Fig. 2 are recovered. The surfactant molecules lead to a high wetting of the continuous phase, since the contact angle of water is around 6° on PDMS and $<5^\circ$ on glass. Therefore, a weak partial wetting of the dispersed phase on the microchannel walls does not preclude the production of fine emulsion drops. Snapshots of the oil jet are reported in Fig. 3a for various flow rate ratios $r_q = q_i / q_o$ that lead to a high lateral confinement of the jet and thus its breakup into monodisperse droplets at the cross-junction. The range of flow rate ratio in Fig. 3a corresponds to the working conditions for this regime. Indeed, if the inner flow rate is decreased, the liquid meniscus enters back into the microchannel. This means that the inner pressure does not overcome the Laplace pressure, that scales like γ / h_1 , to invade the microchannel before the cross-junction and thus to produce droplets. On the other hand, if the inner flow rate is increased, the jet fragmentation results in polydisperse droplets before a transition to a stable two-dimensional jet that breaks at the step as previously discussed. The oil jet is thus fully lubricated by water as sketches in Fig. 3a.

If now a second surfactant is incorporated in the dispersed phase, such as span 80, a partial transient wetting is observed and prevent the formation of fine and calibrated droplets at the step. However, for low flow rate ratios r_q , emulsification at the cross-junction is recovered and exhibits a rich behaviour as reported in Fig. 3. We first note that the contact line of the liquid meniscus is pinned at the end of the inner phase microchannel. Secondly, lower r_q and thus higher lateral confinement of the meniscus than

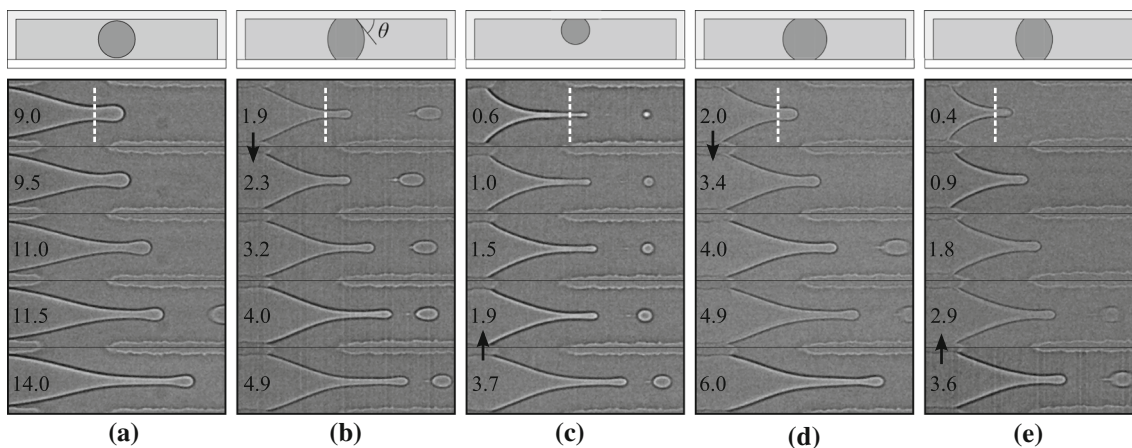


Fig. 3 Meniscus shape as a function of the flow rate ratio $r_q = q_i/q_o$, increasing or decreasing, for various formulations and outer phase flow rates q_o . Non-wetting regime obtained without surfactant in the dispersed phase and with 0.1 wt% of SDS in the continuous phase **a** $q_o = 115$ nl/min. Wetting regime obtained when 1 wt% of span80 is added in the dispersed phase and 0.1 wt% of SDS in the continuous

phase, **b** $q_o = 75$ nl/min for increasing r_q , **c** $q_o = 75$ nl/min for decreasing r_q , **d** $q_o = 235$ nl/min for increasing r_q , **e** $q_o = 235$ nl/min for decreasing r_q . The corresponding flow rate ratio times 100 is reported on each snapshot. The arrows indicate the direction of the variation of r_q . The sketches at the top represent cross-section views of the meniscii at the locations marked by white dashed lines

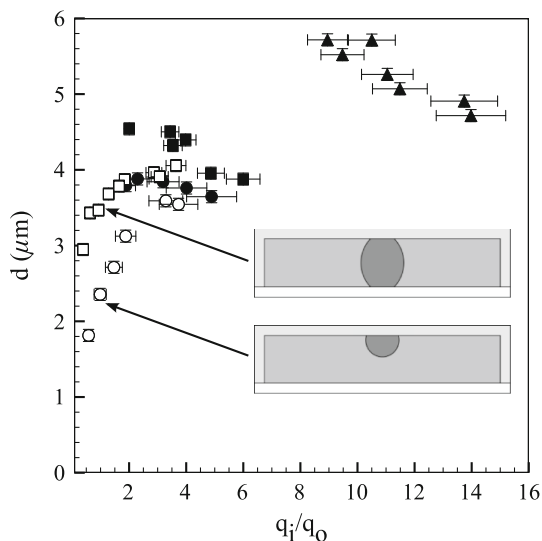


Fig. 4 Evolution of the drop diameter d as a function of the flow rate ratio q_i/q_o when the inner flow rate q_i is first increased (filled symbols) and then decreased (empty symbols) for various formulations and outer phase flow rates q_o : non-wetting regime for $q_o = 115$ nl/min (filled triangle); wetting regime for $q_o = 75$ nl/min (filled circle, open circle); wetting regime for $q_o = 235$ nl/min (filled square, open square). The sketches represent cross-sections of the dispersed phase meniscus when it wets either the two microchannel walls or only one. The drop size measurements correspond to the experiments reported in Fig. 3 for which $h_1 = 1.7$ μm . The error bars on the flow rate ratio come mainly from the accuracy of the continuous flow rate control

the non-wetting case are accessible, as already noticed (Roberts et al. 2012). As a consequence, smaller droplets are produced as shown in Fig. 4. Thirdly, we note an hysteresis of the contact angle that leads to an inversion of the meniscus curvature when r_q is reduced (Fig. 3c, e).

Finally, for the lowest outer flow rate (Fig. 3c) and for the smallest r_q , we observe a very thin meniscus along with a modification of its shape. This indicates a dewetting from one of the two microchannel walls as it has also been reported during bubble formation (Castro-Hernandez et al. 2011). This regime leads to droplet size of the order of the channel height (Fig. 4), here equal to 1.7 μm .

For the experiments reported in Fig. 3, a relatively high concentration of span 80, 1 wt%, is used to ensure wetting of the inner phase at the cross-junction. In addition, the quantity of SDS dispersed in the outer phase is reduced to 0.1 wt% for triggering the oil finger dewetting, and thus its breakup, beyond the cross-junction. Indeed, for an SDS concentration of 1 wt%, the dispersed liquid does not wet the solid walls enough and it is fragmented like in a non-wetting situation. This transient wetting state is therefore achieved by playing with the surfactant concentration C since, for diffusion limited adsorption kinetics, as it is the case for SDS (Bonfillon and Langevin 1993), the characteristic time of surface covering by surfactant molecules varies like $1/C^2$ (Ward and Tordai 1946). Moreover, by changing the outer phase flow rate q_o from 75 to 235 nl/min, we observe a modification of the wetting conditions where the contact line of the meniscus tip is pinned either only at the PDMS wall (Fig. 3c), because plasma treated PDMS is less hydrophilic than glass, or on both glass and PDMS walls (Fig. 3e). This is also a direct consequence of the adsorption kinetics of surfactant molecules at the interfaces, which is frequently encountered in emulsification processes (Lucassen-Reynders and Kuijpers 1992). Indeed, the liquid flow rate sets the characteristic timescale of interfacial area change and velocity at the liquid–liquid

interface. This leads to a transient wetting state that ultimately triggers the dewetting of the meniscus tip followed by its breakup. Obviously, a full description of this emulsification regime should incorporate diffusion and convection of surfactants (Stone 1990).

To conclude, a transient partial wetting of the dispersed phase can be beneficial for the production of fine emulsions in microfluidic systems when the adsorption kinetics of the various surfactants are considered. The drawback of using microsystems built with PDMS is the slow hydrophobicity recovery of the polymeric matrix surface. As a consequence, the experiments are done within one hour for which the wetting condition does not noticeably change.

3.3 Parallelisation: 16 drop makers

The parallelisation of step emulsification process is realised with a microsystem made of 16 drop makers. A partial view of the microfluidic device is shown in Fig. 5. The pressure drop, principally ruled by the smallest channel height, is localised at the cross, and thus all the crosses are linked to the same pressure reservoir. The disparity of the fragmentation features between neighbouring drop generators comes from channel height heterogeneities. The height of the shallow channels shown in Fig. 5 is $2.54 \pm 0.07 \mu\text{m}$. For the least viscous oil, $\eta_i = 1.4 \text{ mPa s}$, the 16 drop makers can all operate in a step emulsification regime with an average frequency of drop formation around 10 kHz. The corresponding yield is 0.22 ml of

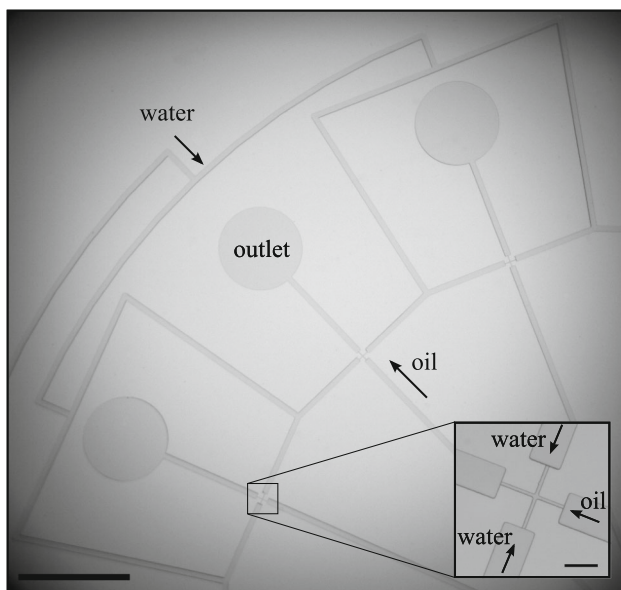


Fig. 5 Partial view of parallelised flow-focusing drop generators with a step. The microfluidic system is composed of 16 drop makers. The scale bar is 2 mm. Inset close view of the cross-junction where the channel depth and width vary from 25 to $2.54 \mu\text{m}$ and from 100 to $10 \mu\text{m}$, respectively. The scale bar is $100 \mu\text{m}$

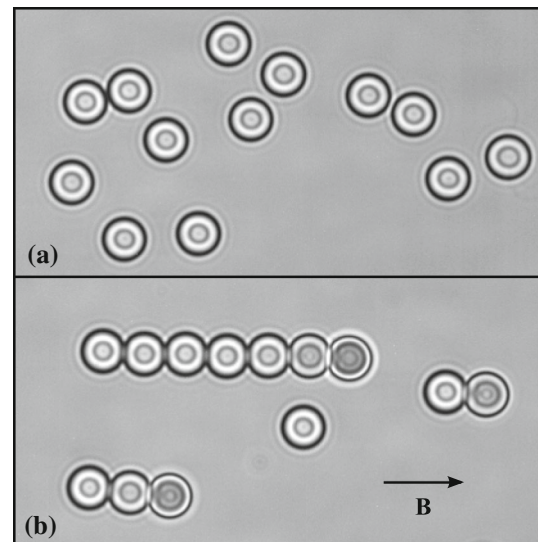


Fig. 6 Droplets of a ferrofluid dispersion **a** without and **b** with magnetic field. The droplet diameter is $6 \mu\text{m}$

droplets per hour having an average diameter of $9 \mu\text{m}$ for an overall polydispersity below 5 %.

In the wetting regime, we operate all the drop generators by first increasing the inner flow rate in order to pin the meniscus contact line while it advances. This precaution is required for working in a fragmentation mode where the droplet size weakly changes with flow rate ratio as compared when the contact line is receding (Fig. 4). Moreover, the range of available flow rate ratios is convenient to parallelise this wetting-assisted emulsification process. This contrasts with the non-wetting regime for which the narrow range of r_q corresponding to a monodisperse dripping regime makes delicate its parallelisation. Indeed, for parallelised systems, only the total flow rates or the upstream pressure of the liquids are controlled but not the local ones that finally shape the emulsion features. We also stress that a double height system, where the drop generator located at the thinner region, is also required for ensuring an efficient parallelisation of droplet production. As stated in the introduction, an interesting feature of emulsions is their capability to encapsulate molecules or particles for creating composite materials that may confer extra properties like the ability to be manipulated under non-hydrodynamic forces. As a proof of concept, superparamagnetic colloidal particles are dispersed in mineral oil resulting in magnetically controllable droplets. Oleic acid, which is used for stabilisation the superparamagnetic nanoparticles, induces a partial wetting of the oil on microchannel walls. The microsystem shown in Fig. 5 has thus been used for emulsifying such a doped oil in a wetting regime. The resulting droplets have a diameter of $6 \mu\text{m}$ as compared to $9 \mu\text{m}$ for a non-wetting condition and in a step emulsification regime. The production yield is around 0.1 ml/h

with a coefficient of variation of the size close to 3 %. Finally, they form chains under magnetic field via induced dipole–dipole interaction as reported in Fig. 6.

4 Conclusion and perspectives

This study shows that a transient partial wetting of the dispersed phase on microsystem walls can be beneficial for making small droplets. This process and the step emulsification one appear to be robust enough for parallelising the droplet production. The parallelisation results to the formation of fine emulsion droplets, diameter below 10 μm , with a narrow size distribution, a polydispersity $<5\%$. The production yield for 16 droplet makers is of the order of 0.1 ml/h. This thus leads to samples whose volumes start to be sufficient for laboratory-scale experiments. We identify two main advantages for using the parallelisation of such a flow configuration. First, the outlets of the drop makers are independent and could thus be discarded if the emulsion feature is not satisfactory. Second, droplet formation is still possible if the dispersed phase partially wets the channel walls. One advantage of making materials by an emulsification step is the possibility to encapsulate molecules or particles that enrich emulsion properties. This feature has been demonstrated by the incorporation of superparamagnetic nanoparticles in the dispersed phase. This results in emulsion droplets that can be manipulated under magnetic field. On the other hand, because of the small channel features, the use of PDMS limits the range of solvents (Lee et al. 2003) that can be handled. Indeed, the PDMS swelling can lead to a collapse of the microchannels that prohibits any liquid flow. Glass devices offer one solution, but are costly. Another viable alternative is to use more solvent resistant polymers such as thiolene-based resins (Cygan et al. 2005). In addition, soft lithography techniques are still possible with these types of UV curable resins (Bartolo et al. 2008) and should thus allow the fabrication of two-layered microsystems. Another drawback of PDMS is the slow hydrophobicity recovery of the polymeric matrix surface that ultimately prohibits the formation of direct emulsion after several hours. This is specially detrimental for the wetting-assisted emulsification regime that might be also overcome utilising the aforementioned materials. However, further investigations are needed for understanding how surfactant transport, surface tension and wetting dynamics as well as fragmentation are coupled.

Acknowledgments We thank Mathilde Reyssat, Florent Malloggi and Rémi Dreyfus for fruitful discussions as well as Fabrice Monti for technical help. This work was supported by the EC-Marie Curie actions and BioMaX (Project Number 264637), and Investissement d’Avenir Program DigiDiag.

References

- Abate AR, Poitzsch A, Hwang Y, Lee J, Czerwinska J, Weitz DA (2009) Impact of inlet channel geometry on microfluidic drop formation. *Phys Rev E* 80(2):026310
- Anna SL, Mayer HC (2006) Microscale tipstreaming in a microfluidic flow focusing device. *Phys Fluids* 18(12):121512
- Anna SL, Bontoux N, Stone HA (2003) Formation of dispersions using “flow focusing” in microchannels. *Appl Phys Lett* 82(3):364–366
- Barbier V, Willaime H, Tabeling P, Jousse F (2006) Producing droplets in parallel microfluidic systems. *Phys Rev E* 74(4):046306
- Bartolo D, Degre G, Nghe P, Studer V (2008) Microfluidic stickers. *Lab Chip* 8(2):274–279
- Bonfillon A, Langevin D (1993) Viscoelasticity of monolayers at oil-water interfaces. *Langmuir* 9(8):2172–2177
- Bremond N, Bibette J (2012) Exploring emulsion science with microfluidics. *Soft Matter* 8(41):10549–10559
- Castro-Hernandez E, van Hoeve W, Lohse D, Gordillo JM (2011) Microbubble generation in a co-flow device operated in a new regime. *Lab Chip* 11(12):2023–2029
- Christopher GF, Anna SL (2007) Microfluidic methods for generating continuous droplet streams. *J Phys D* 40(19):R319–R336
- Cygan ZT, Cabral JT, Beers KL, Amis EJ (2005) Microfluidic platform for the generation of organic-phase microreactors. *Langmuir* 21(8):3629–3634
- Dangla R, Fradet E, Lopez Y, Baroud CN (2013) The physical mechanisms of step emulsification. *J Phys D Appl Phys* 46(11):114003
- Dendukuri D, Doyle PS (2009) The synthesis and assembly of polymeric microparticles using microfluidics. *Adv Mater* 21(41):4071–4086
- Dollet B, van Hoeve W, Raven JP, Marmottant P, Versluis M (2008) Role of the channel geometry on the bubble pinch-off in flow-focusing devices. *Phys Rev Lett* 100(3):034504
- Dreyfus R, Tabeling P, Willaime H (2003) Ordered and disordered patterns in two-phase flows in microchannels. *Phys Rev Lett* 90(14):144505
- Fitch R (1997) *Polymer colloids: a comprehensive introduction*. Academic Press, San Diego
- Ganan-Calvo AM, Gordillo JM (2001) Perfectly monodisperse microbubbling by capillary flow focusing. *Phys Rev Lett* 87(27):274501
- Ganan-Calvo AM, Gonzalez-Prieto R, Riesco-Chueca P, Herrada MA, Flores-Mosquera M (2007) Focusing capillary jets close to the continuum limit. *Nature Phys* 3(10):737–742
- Glotzer SC, Solomon MJ (2007) Anisotropy of building blocks and their assembly into complex structures. *Nat Mater* 6(8):557–562
- Guillot P, Colin A, Utada AS, Ajdari A (2007) Stability of a jet in confined pressure-driven biphasic flows at low reynolds numbers. *Phys Rev Lett* 99(10):104502
- Hong L, Jiang S, Granick S (2006) Simple method to produce janus colloidal particles in large quantity. *Langmuir* 22(23):9495–9499
- Humphry KJ, Ajdari A, Fernandez-Nieves A, Stone HA, Weitz DA (2009) Suppression of instabilities in multiphase flow by geometric confinement. *Phys Rev E* 79(5):056310
- Jeong WC, Lim JM, Choi JH, Kim JH, Lee YJ, Kim SH, Lee G, Kim JD, Yi GR, Yang SM (2012) Controlled generation of submicron emulsion droplets via highly stable tip-streaming mode in microfluidic devices. *Lab Chip* 12(8):1446–1453
- Joscelyne SM, Tragardh G (2000) Membrane emulsification—a literature review. *J Membr Sci* 169(1):107–117
- Kawakatsu T, Kikuchi Y, Nakajima M (1997) Regular-sized cell creation in microchannel emulsification by visual microprocessing method. *J Am Oil Chem Soc* 74(3):317–321

- Kobayashi I, Nakajima M, Chun K, Kikuchi Y, Fukita H (2002) Silicon array of elongated through-holes for monodisperse emulsion droplets. *Aiche Journal* 48(8):1639–1644
- Kobayashi I, Mukataka S, Nakajima M (2005) Novel asymmetric through-hole array microfabricated on a silicon plate for formulating monodisperse emulsions. *Langmuir* 21(17):7629–7632
- Kobayashi I, Wada Y, Uemura K, Nakajima M (2010) Microchannel emulsification for mass production of uniform fine droplets: integration of microchannel arrays on a chip. *Microfluid Nanofluid* 8(2):255–262
- Leal-Calderon F, Schmitt V, Bibette J (2007) *Emulsion science—basic principles*. Springer, Berlin
- Lee JN, Park C, Whitesides GM (2003) Solvent compatibility of poly(dimethylsiloxane)-based microfluidic devices. *Anal Chem* 75(23):6544–6554
- Li W, Nie ZH, Zhang H, Paquet C, Seo M, Garstecki P, Kumacheva E (2007) Screening of the effect of surface energy of microchannels on microfluidic emulsification. *Langmuir* 23(15):8010–8014
- Li W, Greener J, Voicu D, Kumacheva E (2009) Multiple modular microfluidic (m-3) reactors for the synthesis of polymer particles. *Lab Chip* 9(18):2715–2721
- Liabakk NB, Nustad K, Espevik T (1990) A rapid and sensitive immunoassay for tumor necrosis factor using magnetic monodisperse polymer particles. *J Immunol Methods* 134(2):253–259
- Lucassen-Reynders E, Kuijpers K (1992) The role of interfacial properties in emulsification. *Colloids Surf* 65(23):175–184
- Malloggi F, Pannacci N, Attia R, Monti F, Mary P, Willaime H, Tabeling P, Cabane B, Poncet P (2010) Monodisperse colloids synthesized with nanofluidic technology. *Langmuir* 26(4):2369–2373
- Manoharan VN, Elsesser MT, Pine DJ (2003) Dense packing and symmetry in small clusters of microspheres. *Science* 301(5632):483–487
- Margulies M et al (2005) Genome sequencing in microfabricated high-density picolitre reactors. *Nature* 437(7057):376–380
- McDonald JC, Duffy DC, Anderson JR, Chiu DT, Wu HK, Schueller OJA, Whitesides GM (2000) Fabrication of microfluidic systems in poly(dimethylsiloxane). *Electrophoresis* 21(1):27–40
- Nakashima T, Shimizu M, Kukizaki M (2000) Particle control of emulsion by membrane emulsification and its applications. *Adv Drug Deliv Rev* 45(1):47–56
- Nisisako T, Torii T (2008) Microfluidic large-scale integration on a chip for mass production of monodisperse droplets and particles. *Lab Chip* 8(2):287–293
- Olsvik O, Popovic T, Skjerve E, Cudjoe KS, Hornes E, Ugelstad J, Uhln M (1994) Magnetic separation techniques in diagnostic microbiology. *Clin Microbiol Rev* 7(1):43–54
- Priest C, Herminghaus S, Seemann R (2006) Generation of monodisperse gel emulsions in a microfluidic device. *Appl Phys Lett* 88(2):024106
- Roberts CC, Rao RR, Loewenberg M, Brooks CF, Galambos P, Grillet AM, Nemer MB (2012) Comparison of monodisperse droplet generation in flow-focusing devices with hydrophilic and hydrophobic surfaces. *Lab Chip* 12(8):1540–1547
- Romanowsky MB, Abate AR, Rotem A, Holtze C, Weitz DA (2012) High throughput production of single core double emulsions in a parallelized microfluidic device. *Lab Chip* 12(4):802–807
- Rotem A, Abate AR, Utada AS, Van Steijn V, Weitz DA (2012) Drop formation in non-planar microfluidic devices. *Lab Chip* 12(21):4263–4268
- Seo M, Nie ZH, Xu SQ, Mok M, Lewis PC, Graham R, Kumacheva E (2005) Continuous microfluidic reactors for polymer particles. *Langmuir* 21(25):11614–11622
- Shah RK, Kim JW, Agresti JJ, Weitz DA, Chu LY (2008) Fabrication of monodisperse thermosensitive microgels and gel capsules in microfluidic devices. *Soft Matter* 4(12):2303–2309
- Shui LL, van den Berg A, Eijkel JCT (2011) Scalable attoliter monodisperse droplet formation using multiphase nano-microfluidics. *Microfluid Nanofluid* 11(1):87–92
- Song H, Chen DL, Ismagilov RF (2006) Reactions in droplets in microfluidic channels. *Angew Chem Int Ed* 45(44):7336–7356
- Stone HA (1990) A simple derivation of the time-dependent convective-diffusion equation for surfactant transport along a deforming interface. *Phys Fluids A-Fluid Dyn* 2(1):111–112
- Sugiura S, Nakajima M, Kumazawa N, Iwamoto S, Seki M (2002) Characterization of spontaneous transformation-based droplet formation during microchannel emulsification. *J Phys Chem B* 106(36):9405–9409
- Tawfik DS, Griffiths AD (1998) Man-made cell-like compartments for molecular evolution. *Nat Biotechnol* 16(7):652–656
- Tetradis-Meris G, Rossetti D, de Torres CP, Cao R, Lian GP, Janes R (2009) Novel parallel integration of microfluidic device network for emulsion formation. *Ind Eng Chem Res* 48(19):8881–8889
- Theberge AB, Courtois F, Schaeferli Y, Fischlechner M, Abell C, Hollfelder F, Huck WTS (2010) Microdroplets in microfluidics: an evolving platform for discoveries in chemistry and biology. *Angew Chem Int Ed* 49(34):5846–5868
- van Dijke K, Veldhuis G, Schroen K, Boom R (2009) Parallelized edge-based droplet generation (edge) devices. *Lab Chip* 9(19):2824–2830
- Vladisavljevic GT, Duncanson WJ, Shum HC, Weitz DA (2012a) Emulsion templating of poly(lactic acid) particles: Droplet formation behavior. *Langmuir* 28(36):12948–12954
- Vladisavljevic GT, Kobayashi I, Nakajima M (2012b) Production of uniform droplets using membrane, microchannel and microfluidic emulsification devices. *Microfluid Nanofluid* 13(1):151–178
- Vyawahare S, Griffiths AD, Merten CA (2010) Miniaturization and parallelization of biological and chemical assays in microfluidic devices. *Chem Biol* 17(10):1052–1065
- Wang ZF, Guo HS, Yu YL, He NY (2006) Synthesis and characterization of a novel magnetic carrier with its composition of Fe₃O₄/carbon using hydrothermal reaction. *J Magn Magn Mater* 302(2):397–404
- Ward AFH, Tordai L (1946) Time-dependence of boundary tensions of solutions i. the role of diffusion in time-effects. *J Chem Phys* 14(7):453–461
- Zerrouki D, Baudry J, Pine D, Chaikin P, Bibette J (2008) Chiral colloidal clusters. *Nature* 455(7211):380–382